ACS APPLIED MATERIALS & INTERFACES

Research Article

www.acsami.org

Alternative Carrier Injection/Extraction Inspired by Electrode Interlayers Based on Peripheral Modification of the Electron-Rich Skeleton

Dongcheng Chen, Chongyang Zhang, Hu Zhou, Xinchao Li, Zhiheng Wang, Shi-Jian Su,* and Yong Cao

State Key Laboratory of Luminescent Materials and Devices and Institute of Polymer Optoelectronic Materials and Devices, South China University of Technology, Guangzhou 510640, China

Supporting Information

ABSTRACT: Peripheral modifications of the electron-rich trifluorene-substituted triphenylamine core have been comparatively studied through the linkage of the different polar pendants with fluorene via saturated sp^3 hybrid alkyl chains. The work function of electrode could be effectively tuned by the interlayers with or without peripheral pendants of phosphoric acid and phosphonate groups to give selective hole and electron injection/extraction property. Their applications in various vacuum- and solution-processed organic light-emitting diodes and photovoltaic devices were thoroughly investigated. The current comparative study provides valuable exploration on developing high-performance environmentally friendly solvent-processed electrode interlayer materials.

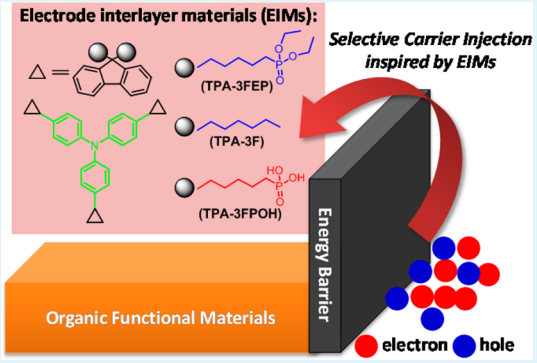

KEYWORDS: *carrier injection/extraction, organic/polymer light-emitting diodes, polymer solar cells, environment-friendly, electrode interlayers*

INTRODUCTION

Organic optoelectronic devices have attracted extensive attention during recent decades. Among them, organic light-emitting diodes (OLEDs) and organic photovoltaic devices (OPVs) are the most extensively researched ones. As is widely known, a well-modified electrode/organic contact interface is of comparable importance to rational selection of active layer materials and carrier transport materials. It is known that for OLEDs carrier injection is the first step in the electricity to light conversion procedure, which is a prerequisite to the sequential carrier transport and exciton radiative decay processes. As for OPVs, carrier extraction at the organic/electrode interface is the last step for the light to electricity conversion procedure; however, it is also one vital step to determine how well the current and voltage are extracted. Noting that the commonly used electrode materials are difficult to meet the requirements for efficient carrier injection/extraction due to their unmatched energy level alignment with the bulky organic materials, thereby modification of the electrode by the interlayer materials is often needed to tune their carrier injection/extraction abilities.

ITO (indium tin oxide) is commonly adopted as an anode material for hole injection/extraction in organic optoelectronic devices, due to its high transmission for visible light and high conductivity. However, owing to its relatively low work function in the range from −4.5 to −4.7 eV,[1,2] an energy difference between the Fermi energy level of ITO and the highest occupied molecular orbital (HOMO) energy level of the bulky organic materials generally exists, which would reduce its hole injection/extraction abilities. A widely adopted strategy is to make an anode buffer layer atop ITO to help selective hole injection/extraction. PEDOT:PSS is one of the most adopted hole-selective materials for both OLEDs and OPVs owing to its increased effective work function, good water-processed ability, and high transmission. However, it has been demonstrated that PEDOT:PSS on ITO is unstable, because indium atoms can contaminate the polymer.[3,4] The acid nature of PEDOT:PSS can also be harmful to the organic active layer, thus degrading the long-term device performance.[5] Many other hole-selective materials, like alcohol-processed molecules,[6] solution-processed p-doping polymers,[7,8] and inorganic metal oxides,[9] have been investigated and show improved hole injection/extraction ability compared to the bare ITO anode. The inverted device structures in which ITO is utilized as a cathode are also helpful to avoid the above shortages of PEDOT:PSS atop ITO.[10,11] Similar unmatched energy level alignment is also found in the case of interfacial contact between the commonly used stable cathode metals like Al and the lowest occupied molecular orbital (LUMO) energy level of the bulky organic materials. A cathode interlayer to assist electron injection/extraction from/to the cathode is, thus, also equally important to the anode interlayer. Low work function metals, metal fluorides and carbonates, are usually vacuum evaporated as electron-selective

Received: October 26, 2014
Accepted: January 21, 2015
Published: January 21, 2015

DOI: 10.1021/am507429j
ACS Appl. Mater. Interfaces 2015, 7, 3133−3141

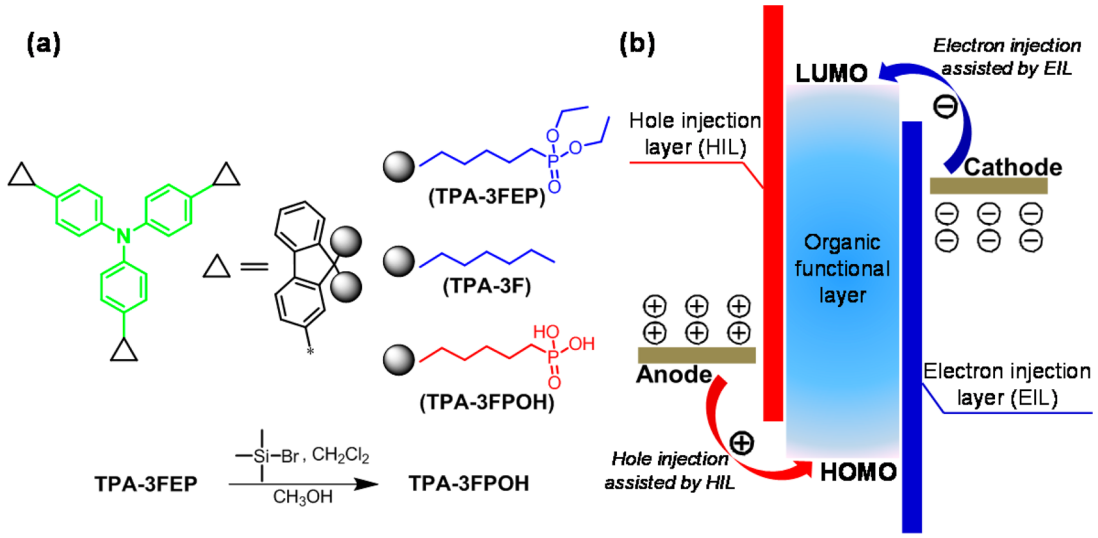

Figure 1. (a) Molecular structures of the investigated materials of TPA-3FPOH, TPA-3F, and TPA-3FEP, and the one-step synthetic route from TPA-3FEP to TPA-3FPOH. (b) Sketch map of the hole and electron injection from the corresponding electrodes to the organic functional layer assisted by the hole and electron injection layer.

layers to form Ohmic contacts between the cathode and the bulky organic materials, however, limiting their applications in solution-processed organic optoelectronic devices. Solution-processed polymer and small molecule-based electron-selective materials have been developed and demonstrated their effectiveness in injecting and extracting electrons in OLEDs and OPVs.[12−16] Linkage of a conjugated backbone with polar side chains has been a widely adopted strategy to develop carrier-selective materials for both holes and electrons. Several mechanisms like interfacial dipole-induced better carrier injection,[12,17,18] electron transfer between the ammonium-based interlayer and the n-type fullerenes,[19] and combined interfacial dipole effect and intense coordination interaction between Al and the phosphonate groups[20] have been demonstrated to explain the observed enhancement in device performance using these interlayer materials. Some issues correlating to the relationships of the structure and the property for these interlayer materials still remain, e.g., it is still difficult to tell how the nature of the conjugated backbone functions in the carrier injection or extraction process. Further work to increase our knowledge about the interlayer materials is still deserved.

In this work, we provide a comparative study on hole- and electron-selective materials based on an identical trifluorene-substituted triphenylamine core which is of hole-transport property in nature with or without peripheral pendants of phosphoric acid or phosphonate groups (Figure 1a). It was found that the peripheral groups have a great effect on its solubility in different organic solvents and electron/hole injection/extraction abilities. The molecule, namely, TPA-3F, having no polar unit on the periphery, is of good solubility in weak polar organic solvents and could be used as a good hole transport material. However, its good solubility in common weak polar organic solvents and weak work function tuning ability limit its application as a good hole injection material for solution-processed organic optoelectronic devices. An effective strategy toward a good solution-processed hole injection material is demonstrated here, by linkage of the TPA-3F moiety and several polar phosphoric acid groups on the periphery to give a new hole injection/extraction material, namely, TPA-3FPOH. Efficient hole injection and extraction is achieved when TPA-3FPOH is used as an anode buffer layer for both solution-processed and vacuum-fabricated organic optoelectronic devices. Interestingly, TPA-3FEP combining the TPA-3F moiety and the peripheral phosphonate units exhibits contrasting electron injection/extraction property, which demonstrated its effectiveness as a cathode interlayer for the solution-processed organic light-emitting and photovoltaic devices. The current developed interlayer materials could also find their potential applications in other organic optoelectronic devices, like photodetectors and field effect transistors. These findings have important significance for developing high-performance electrode interlayer materials and may help to know more about the original working principles of the electrode interlayer.

EXPERIMENTAL SECTION

Material Synthesis and Characterization. All of the reagents and solvents used for syntheses were purchased from Alfa Aesar or Acros and used as received. All of the reactions were performed under a dry-nitrogen atmosphere. ^{1}H and ^{13}C NMR spectra were recorded on a Bruker AV-300 spectrometer operating at 300 and 75 MHz, respectively, at 298 K using deuterated chloroform ($CDCl_3$) or deuterated water (D_2O) as the solvent and tetramethylsilane (TMS) as the internal standard. The mass spectrum (MS) was recorded on a Bruker Esquire HCT PLUS with an electrospray ionization (ESI) resource. Differential scanning calorimetry (DSC) was performed with a Netzsch DSC 204 under a nitrogen atmosphere at a heating rate of 10 °C min^{-1}. UV−vis absorption spectra were recorded on a HP 8453 spectrophotometer. Cyclic voltammetry (CV) was carried out on a CHI660D electrochemical workstation with a platinum working electrode and a platinum wire counter electrode at a scan rate of 50 mV s^{-1} against the saturated calomel electrode (SCE) reference electrode with an argon-saturated solution of tetrabutylammonium hexafluorophosphate (Bu_4NPF_6) (0.1 mol L^{-1}) in anhydrous acetonitrile.

Synthesis of TPA-3FEP and TPA-3F can be found in the literature.[15] (((Nitrilotris(benzene-4,1-diyl))tris(9*H*-fluorene-9,9,2-triyl))hexakis(hexane-6,1-diyl))hexaphosphonic acid (TPA-3FPOH) was obtained by a one-step reaction from TPA-3FEP (Figure 1a). Its UV−vis absorption and photoluminescent (PL) spectra are shown in Figure S1 (see Supporting Information). Compound TPA-3FEP (0.3492 g, 0.170 mmol) was dissolved in dry dichloromethane (DCM)

DOI: 10.1021/am507429j
ACS Appl. Mater. Interfaces 2015, 7, 3133−3141

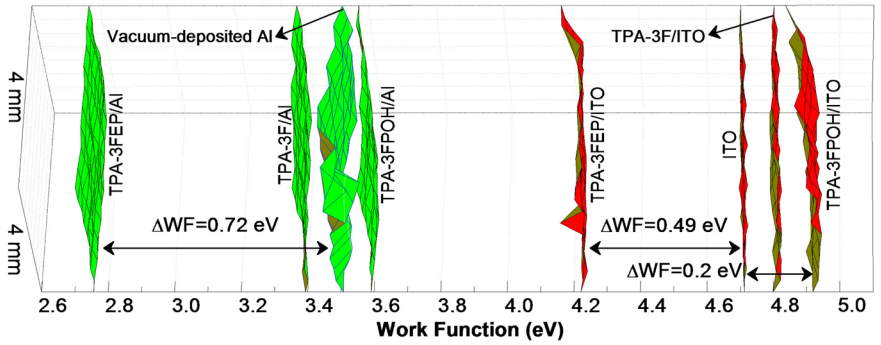

Figure 2. Work function measurement on a square area (4 mm × 4 mm) of the ITO and Al substrates with or without a 5 nm thin modified interlayer of TPA-3F, TPA-3FEP, or TPA-3FPOH by scanning Kelvin probe in a N_2 atmosphere.

solvent, and then bromotrimethylsilane (1.5 mL, 11.4 mmol) was added dropwise. The reaction mixture was stirred at room temperature for 24 h. After removing the solvent, 40 mL of DCM and methanol (1:3) was added and stirred for another 24 h. The crude product was then filtrated, dried, and washed by acetonitrile twice to give a yellow solid in 95.4% yield. ^{1}H NMR (300 MHz, CD_3OD): δ (ppm) 7.68−7.52 (m, 6H), 7.35−7.16 (m, 5H), 2.03 (m, 4H), 1.49−1.36 (m, 8H), 1.03−0.80 (m, 8H), 0.60 (m, 8H). ^{31}P NMR (DMSO, 121 MHz): δ (ppm) −28.02. MALDI-TOF MS: m/z = 1722.84.

Device Fabrication and Characterization. The ITO-coated glass substrates were cleaned in sequence in an ultrasonic bath of acetone, detergent, deionized water, and isopropyl alcohol and then dried in an oven at 80 °C for more than 2 h. Before the start of device fabrication, the clean ITO substrates were treated with O_2 plasma for 20 min. The PEDOT:PSS (Baytron P4083, Bayer AG) layer was spin coated in the air and then transferred to the glovebox to be heated at 120 °C for 30 min. All other solution-processed organic layers were spin coated in the glovebox with a N_2 atmosphere at room temperature. TPA-3FPOH and TPA-3FEP were dissolved and processed in their methanol solutions, whereas TPA-3F, which cannot be dissolved in polar solvent, was processed from its toluene solution. After deposition of the TPA-3FPOH, TPA-3FEP, or TPA-3F layer, the substrates were heated at 80 °C for 10 min to remove the residual solvent. *p*-Xylene was used as the solvent for spin coating the poly[2-(4-(3′,7′)-dimethyloctyloxy)phenyl]-*p*-phenylenevinylene] (P-PPV) layer. Chlorobenzene was used as the solvent for spin coating the poly(*N*-vinyl-carbazole) (PVK) layer, iridium(III) bis(4,6-(difluorophenyl)pyridinato-N,$C^{2'}$) picolinate (FIrpic)-containing the light-emitting layer (PVK:1,3-bis[(4-*tert*-butylphenyl)-1,3,4-oxadiazolyl]phenylene (OXD-7):FIrpic = 70:30:10, weight ratio), and poly[*N*-9″-heptadecanyl-2,7-carbazole-*alt*-5,5-(4′,7′-di-2-thienyl-2′,1′,3′-benzothiadiazole)] (PCDTBT):[6,6]-phenyl C_{71}-butyric acid methyl ester ($PC_{71}BM$) (1:4, weight ratio) the photovoltaic active layer. Tris(8-hydroxy-quinoline) aluminum (Alq3) and 10-(2-benzothiazolyl)-2,3,6,7-tetrahydro-1,1,7,7-tetramethyl-1*H*,5*H*,11*H*-(1)-benzopyropyrano(6,7−8-*I*,*j*) quinolizin-11-one (C545T) were vacuum deposited at a rate of 0.1−0.2 nm s^{-1} under a base pressure below 5 × 10^{-4} Pa, and then LiF and Al with an area of 0.09 cm^2 were deposited as a cathode for these devices. Ba/Al or Al were vacuum deposited as a cathode with an area of 0.15 cm^2 for solution-processed light-emitting and photovoltaic devices under a base pressure of 1 × 10^{-4} Pa. Single-carrier devices were fabricated with similar procedures. PVK and $PC_{71}BM$ were purchased from Sigma-Aldrich. PCDTBT was purchased from 1-material Chemscitech Inc. (St-Laurent, Quebec, Canada). Other commercial organic materials like FIrpic, OXD-7, Alq3, and C545T were purchased from Luminescence Technology Corp. (Lumtec, Taiwan). All commercial materials were used as received without further purification.

Profilometry (Veeco Dektak 150) was used to determine the thickness of the solution-processed organic layer, except that the thicknesses of those ultrathin organic layers of about 5 nm were estimated from their absorption intensity compared to their thick layers with a thickness determined by Veeco Dektak 150. The thicknesses of the vacuum-deposited organic layers and the cathode were monitored upon deposition by using a crystal thickness monitor (Sycon) and calibrated by Veeco Dektak 150. Apart from cleaning ITO and spin-coating PEDOT:PSS, device fabrication was carried out in a N_2 atmosphere drybox (Vacuum Atmosphere Co.). Current density−voltage−luminance (J−V−L) characteristics of the solution-processed light-emitting devices were measured using a Keithley 236 source meter and a calibrated silicon photodiode. Luminance was calibrated by a spectrophotometer (Photo Research, model SpectraScan PR-705), and the electroluminescent (EL) spectrum and Commission International de l'Eclairage (CIE) coordinates were simultaneously obtained. J−V−L characteristics of the vacuum-fabricated OLEDs were measured by a Keithley source-measure unit 2400 and Konica Minolta chromameter CS-200. Photovoltaic measurement was carried out under an AM 1.5G solar simulator (Oriel model 91192). The power of sun simulation was calibrated to be 1000 W m^{-2} before testing using a standard silicon solar cell. Scanning Kelvin probe (SKP) measurement was carried out on a SKP 5050 (KP Technology) in a N_2 atmosphere.

RESULTS AND DISCUSSION

Work Function Measurement. Work function measurement was conducted on two widely used anode and cathode materials of ITO and Al. All fabrication and measurement process were conducted in a N_2 atmosphere to minimize the potential effect of the environment. As shown in Figure 2 and Table 1, the work function of the pristine ITO is 4.71 ± 0.02 eV, which is quite consistent with the values reported in the literature.[1,2] When it is coated by a thin layer of TPA-3F, the variation of their effective work function is inconspicuous (4.81 ± 0.02 eV), suggesting that TPA-3F has a weak ability to tune the work function of the ITO substrate. In contrast, incorporation of a thin film of TPA-3FPOH results in a slight increase to 4.91 ± 0.07 eV, which is on average about 0.2 eV higher than that of the pristine ITO. This result is a bit different from the case of the reported self-assembled monolayers (SAMs) based on triphenylamine and phosphoric acid groups, which may result from their different molecular structure and film-forming method.[21] Further investigation of the adsorption

Table 1. Summary of the Work Function Values (eV) of the ITO and Al Substrates with or without a 5 nm Thin Modified Interlayer of TPA-3F, TPA-3FEP, or TPA-3FPOH, Measured by Scanning Kelvin Probe in a N_2 Atmosphere

electrode	pristine	with TPA-3FPOH	with TPA-3F	with TPA-3FEP
ITO	4.71 ± 0.02	4.91 ± 0.07	4.81 ± 0.02	4.22 ± 0.05
Al	3.50 ± 0.07	3.59 ± 0.04	3.39 ± 0.02	2.77 ± 0.02

DOI: 10.1021/am507429j
ACS Appl. Mater. Interfaces 2015, 7, 3133−3141

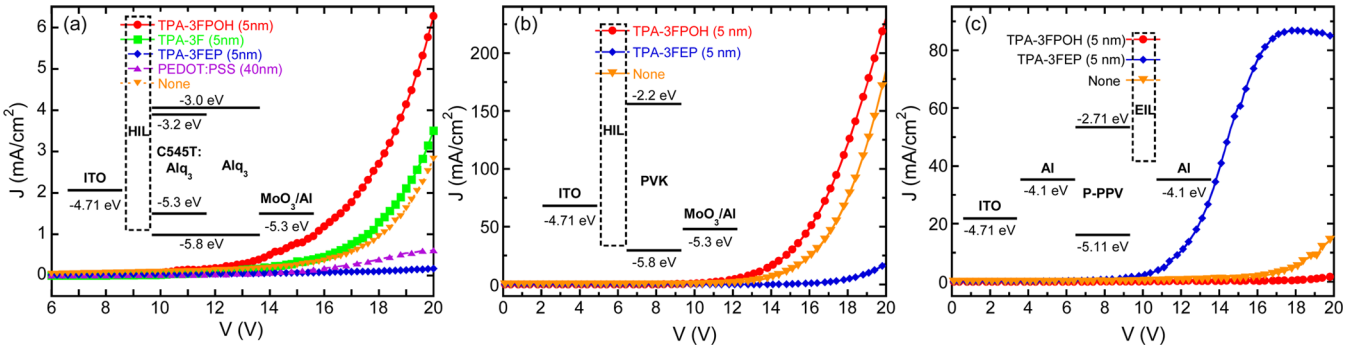

Figure 3. Current density−voltage (J−V) characteristics of the single-carrier devices. Hole-only devices with a configuration of ITO/HIL/organic functional layer/MoO_3 (10 nm)/Al (100 nm); the organic functional layer is (a) C545T (3 wt %):Alq3 (30 nm)/Alq3 (40 nm) and (b) PVK (100 nm). Electron-only devices with a configuration of ITO/Al (40 nm)/P-PPV (100 nm)/EIL (5 nm)/Al (100 nm) (c).

property of TPA-3FPOH on the ITO substrate will be carried out in our future work according to the established methods.[22−24] However, when the TPA-3FEP thin film is atop, their effective work function shows a more pronounced decrease of 0.49 eV, giving a value of 4.22 ± 0.05 eV. Generally, to achieve efficient hole injection from the anode to the HOMO energy level of the organic functional layer (commonly hole transport layer (HTL)), a reduced energy barrier between the anode and the HTL is preferred (Figure 1b). Therefore, if used as an anode buffer layer, it is speculated that more efficient hole injection/extraction could be obtained by TPA-3FPOH, which has a relatively deep work function compared with the other two. Besides, the HOMO level of TPA-3FPOH (5.04 eV, Figure S2, See Supporting Information) is deeper than the work function of ITO, which is also beneficial to improve hole injection/extraction from/to the ITO anode. Due to its worse solubility in weak polar organic solvents, its functionality as an anode buffer layer for solution-processed organic optoelectronic devices is also anticipated.

Another set of work function measurement was carried out on the vacuum-deposited Al substrate. The pristine deposited Al shows a work function of 3.49 ± 0.07 eV, which is about 0.6 eV lower than the clean Al. This is probably attributed to the unavoidable partial oxidation of Al surface.[25] An additional thin layer of TPA-3F or TPA-3FPOH on the Al substrate leads to a small work function variation of ca. 0.1 eV. However, TPA-3FPOH has a tendency to increase it, and TPA-3F slightly decreases it. Nevertheless, it reveals that both TPA-3F and TPA-3FPOH weakly affect the work function of the Al cathode. However, a dramatic decrease of the work function of 0.72 eV was observed for TPA-3FEP atop the Al substrate, yielding an effective work function of 2.77 ± 0.02 eV. Thus, it suggests that TPA-3FEP should be a good candidate to serve as a cathode interlayer to achieve efficient electron injection or extraction from a stable metal electrode like Al, and this has been initially demonstrated on the green polymer light-emitting devices (PLEDs) and the polymer solar cells.[15] The dramatically reduced effective work function of the TPA-3FEP/Al cathode may originate from the combined effect of the interfacial dipole[12] and the coordination interaction between the phosphonate units and Al.[20]

Carrier-Selective Injection. In order to further investigate the carrier-selective injection abilities of these materials, a series of single-carrier devices has been fabricated to compare their current density−voltage characteristics. For the hole-only devices, electrons are mostly blocked outside the external circuit. Thus, the discrepancy of the device current densities could be ascribed to the different hole flux induced by the various injection abilities of the used anode buffer layer. The same goes for the electron-only devices. Hole-only devices were first testified in a configuration of ITO/HIL/C545T (3 wt %):Alq3 (30 nm)/Alq3 (40 nm)/MoO_3 (10 nm)/Al (100 nm), where HIL differs in TPA-3FPOH (5 nm), TPA-3F (5 nm), TPA-3FEP (5 nm), PEDOT:PSS (40 nm), and none (bare ITO as an anode). As shown in Figure 3a, the device based on TPA-3FPOH shows the highest current density among these hole-only devices from 11 to 20 V. In contrast, a reduced current density is observed for the device based on TPA-3F. However, it is still higher than that of the devices with no anode buffer layer or using PEDOT:PSS as an anode buffer layer. Inversely, the device based on TPA-3FEP exhibits the smallest current density, which is lower than those of the devices based on TPA-3FPOH and TPA-3F and even worse than those of the devices with no anode buffer layer or using PEDOT:PSS as an anode buffer layer. The solution-processed device based on PEDOT:PSS had small hole current density here, which may originate from its bigger bulky resistance. It is worth noting that C545T:Alq3/Alq3 is a system beneficial for electron transport, whereas the low electron mobility of Alq3 (1.4×10^{-6} cm^2 V^{-1} s^{-1})[26] presumably leads to a small current density for these devices (below 10 mA cm^{-2} within 20 V). Thus, we further promote the hole-only devices in a hole transport system, which is comprised of a PVK layer (Figure 3b). PVK is of hole transport property in nature; however, its deep HOMO energy level can cause a difficulty in hole injection from the ITO anode. As can be seen, combination of a thin TPA-3FPOH layer on the ITO anode induces an enhanced hole flux compared to the bare ITO anode. In contrast, though it may be washed out partly by the subsequently used solvent, the residual TPA-3FEP layer still leads to a dramatically reduced hole current density in the PVK-based devices.

From the above discussion, one may conclude that TPA-3FPOH is a material that could be utilized as an anode buffer layer to help hole injection for both vacuum- and solution-processed optoelectronic devices. However, TPA-3FEP, which had a bad hole injection ability, inversely, would prevent hole injection from the anode. Note that those trifluorene-substituted triphenylamine derivatives have a HOMO energy level at around 5.0 eV (Figure S2, Supporting Information),[27] which are quite suitable for hole injection. However, the peripheral units at the end of the *n*-hexyls combined with the fluorene moiety play an important role in tuning the work function of the anode, which also affects their hole injection utilities. As aforementioned, TPA-3FPOH causes a 0.2 eV

DOI: 10.1021/am507429j
ACS Appl. Mater. Interfaces 2015, 7, 3133−3141

increased work function compared to the bare ITO substrate. The combined effects of an increased work function of the anode and the appropriate HOMO energy level for TPA-3FPOH result in the largest hole flux in the hole-only devices based on C545T:Alq3/Alq3 or PVK. TPA-3F, without any polar units on the periphery, causes a slight variation of the ITO work function, whereas its matched HOMO energy level contributes to the hole injection. As a result, in contrast to the bare ITO as an anode, enhanced hole flux was also observed for the hole-only device using TPA-3F as a buffer layer. As for TPA-3FEP, it lowers the work function of the ITO substrate to 4.22 eV, leading to a big hole injection barrier from the anode. Thus, incorporation of TPA-3FEP onto the ITO anode leads to the worst hole current density among all the fabricated hole-only devices.

Electron-only devices were fabricated with a structure of ITO/Al (40 nm)/P-PPV (100 nm)/EIL/Al (100 nm), where EIL differs in TPA-3FPOH (5 nm), TPA-3FEP (5 nm), none (bare Al as a cathode). TPA-3F was not investigated in this configuration, because it cannot be wet processed by orthonormal solvent like alcohol. Furthermore, one can anticipate the bad performance of TPA-3F when used as a cathode interlayer, due to its electron-rich nature and weak work function tuning ability. Figure 3c depicts the current density−voltage characteristics of these electron-only devices. It was observed that TPA-3FEP dramatically enhanced the electron flux while being employed as a cathode interlayer, relative to the device using bare Al as a cathode. This could be ascribed to the lower effective work function of TPA-3FEP/Al compared to bare Al, which reduces the electron injection barrier between the cathode and the LUMO energy level of P-PPV and thus leads to an improved electron injection current. A reduced electron current density was observed for the device based on TPA-3FPOH/Al at high electric field, which could also be attributed to the injection barrier variation due to the increased work function compared to the bare Al cathode.

Light-Emitting and Photovoltaic Device Applications. *Anode Interlayers for Light-Emitting Devices.* The 10 nm thin MoO_3 layer was removed from the hole-only devices based on C545T:Alq3/Alq3. Instead, a 1 nm thin LiF layer was incorporated as an electron injection layer to give light-emitting devices. It is worth noting that C545T:Alq3/Alq3 is a system favorable for electron transport. Enhancement of the hole current density and blocking of the electron flux in the devices comprised of this system would lead to obviously discrepant device performances. Thus, it provides a good platform to investigate the anode interlayer materials with different hole injection and electron blocking abilities. Besides, because TPA-3F was anticipated with good hole transport performance, it was also utilized as a hole transport material within the device with TPA-3FPOH as a hole injection layer (HIL).

As shown in Figure 4a, though a similar operating current density was observed for the device based on TPA-3FPOH and the reference device without HIL, the operating voltages for the device using TPA-3FPOH as a HIL are much lower than those of the reference device with a bare ITO anode, and the maximal current efficiency (CE) of the former device is about 3 times higher than that of the bare ITO device (9.43 vs 3.50 cd A^{-1}). It is deduced the bare ITO device with the absence of HIL may lead to difficult hole injection, weak electron blocking, and thus leakage current, mostly induced by excess electron flux originating from the electron transport nature of the C545T:Alq3/Alq3 system, and this is responsible for the

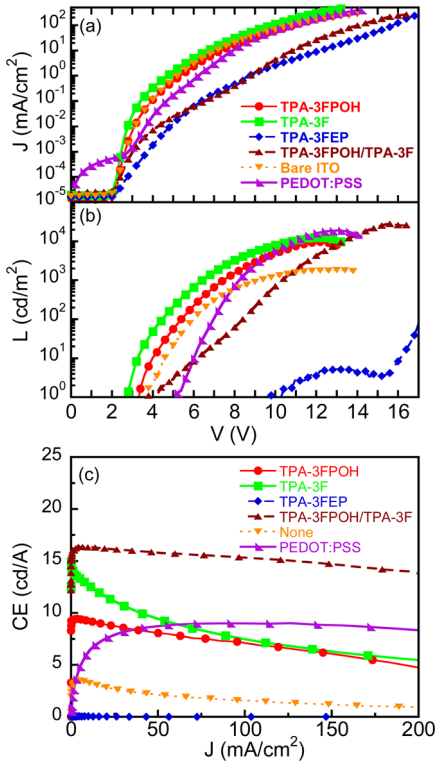

Figure 4. (a) Current density−voltage (J−V), (b) luminance−voltage (L−V), and (c) current efficiency−current density (CE−J) characteristics of the devices with a configuration of ITO/HIL/C545T:Alq3 (30 nm)/Alq3 (40 nm)/LiF (1 nm)/Al (100 nm), where HIL differs in TPA-3FPOH (5 nm), TPA-3F (5 nm), TPA-3FEP (5 nm), combined TPA-3FPOH (5 nm)/TPA-3F (40 nm), none (bare ITO as an anode), and PEDOT:PSS (40 nm).

relatively large operating current and low current efficiency due to the unbalanced carrier recombination. As confirmed by the former hole-only devices, incorporation of a 5 nm thin TPA-3FPOH as a HIL made the hole injection easier to give more balanced hole and electron recombination within the emissive layer (EML), and a lower operating voltage and higher efficiency was thus obtained. In contrast to the device based on PEDOT:PSS, the device based on TPA-3FPOH exhibited higher efficiency at low luminance and, however, lower efficiency at high electric field. This indicates that the working mechanism for TPA-3FPOH to help hole injection is different from the p-doping PEDOT:PSS. The device containing an additional layer of 40 nm thin TPA-3F between the TPA-3FPOH layer and the EML exhibited much higher efficiency (a maximal CE value of 16.3 cd A^{-1}). Considering the LUMO energy level of TPA-3F is 2.07 eV, which is about 1 eV higher than the LUMO energy level of Alq3, a relatively thick TPA-3F layer could block the electron leakage flux, and the combined hole injection and electron blocking abilities of ITO/TPA-3FPOH (5 nm)/TPA-3F (40 nm) made the device thereof have balanced carrier recombination and higher efficiency. It is also worth noting that the HOMO energy level of 5.0 eV for TPA-3F is also suitable to assist the hole injection from the ITO anode. The device containing a 5 nm thin TPA-3F layer also achieved quite low operating voltages and quite high efficiency (a maximal CE value of 15.0 cd A^{-1}). This might be ascribed to its good hole injection and electron blocking properties, which is similar to the traditional arylamine-based hole injection and transport materials, e.g., 4,4′-bis(*N*-(1-

DOI: 10.1021/am507429j
ACS Appl. Mater. Interfaces 2015, 7, 3133−3141

naphthyl)-*N*-phenylamino)biphenyl (NPB). However, due to the excellent solubility of TPA-3F in common organic solvents, the application of TPA-3F in solution-processed optoelectronic devices is limited. The effective reduction of work function of the ITO anode by TPA-3FEP with the phosphonate units resulted in a big hole injection barrier, and the hole injection from this bilayer anode was difficult; therefore, the device containing ITO/TPA-3FEP (5 nm) showed dramatically large driving voltages and much lower efficiency with CE values below 0.1 cd A^{-1}.

Anode Buffer Layers for Photovoltaic Devices. It has been testified that TPA-3FPOH should have a good hole injection ability for application in vacuum-fabricated OLEDs. Due to its worse solubility in common weak polar organic solvents, TPA-3FPOH could also be used as an anode interlayer material to assist hole injection/extraction for solution-processed optoelectronic devices. The effectiveness of TPA-3FPOH as a hole extraction layer was also evaluated in wet-processed organic photovoltaic devices in a device configuration of ITO/TPA-3FPOH (5 nm), PEDOT:PSS (40 nm), or no hole extraction layer/PCDTBT:$PC_{71}BM$ (1:4 in weight, 80 nm)/Al (100 nm). After deposition of the active layer, methanol was spin coated atop the active layer. As shown in Figure 5, in contrast to the control device with no hole extraction layer, the TPA-3FPOH-containing device exhibited simultaneously enhanced open-circuit voltage (V_{oc}), short-current density (J_{sc}), and fill factor (FF), resulting in the enhanced power conversion efficiency (PCE) (6.10% vs 4.94%). The improvement of the device performance should originate from the tuned work function of the ITO anode coated by TPA-3FPOH, thereby, increasing the hole extraction ability. The device based on TPA-3FPOH gave a V_{oc} of 0.94 V, which is very close to that of the traditional device based on PEDOT:PSS, and a J_{sc} of 11 mA cm^{-2}, which is larger than that of the device containing PEDOT:PSS. Due to the compromised FF of 58.98% (vs 63.22%), a slightly lower PCE of 6.10% was achieved for the device based on TPA-3FPOH, as compared to that of 6.32% for the PEDOT:PSS-based device. This indicates that TPA-3FPOH can be used as an efficient hole extraction material for solution-processed organic photovoltaic devices. It is noted that utilization of TPA-3FPOH as a HIL for solution-processed P-PPV-based PLEDs has also been testified (not shown here), giving a similar significantly enhanced performance relative to the device with no HIL and comparable device performance in contrast to the device using PEDOT:PSS as a HIL.

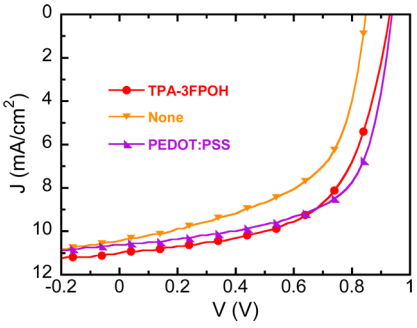

Figure 5. Current density−voltage (J−V) characteristics of the organic photovoltaic devices with or without hole extraction layers measured under 1000 W m^{-2} AM 1.5 G illumination. Device configuration is ITO/TPA-3FPOH (5 nm), PEDOT:PSS (40 nm), or no hole extraction layer/PCDTBT:$PC_{71}BM$ (1:4 in weight, 80 nm)/Al (100 nm).

Cathode Buffer Layers for Light-Emitting Devices. As previously demonstrated by work function measurement and single-carrier devices, TPA-3FEP having a trifluorene-substituted triphenylamine core and the peripheral phosphonate pendants could have excellent electron injection/extraction abilities. These conclusions have been verified by applying TPA-3FEP as a cathode interlayer in green PLEDs and in organic solar cells.[15] Further investigation found that TPA-3FEP could also be utilized as a light-emitting material to build up efficient cathode-interlayer-free blue OLEDs by solution processing.[27] We promote the experiment to assess the thickness-dependent electron injection ability of TPA-3FEP in a device configuration of ITO/PEDOT:PSS (40 nm)/P-PPV (85 nm)/TPA-3FEP (x nm, x = 5, 16, 42, 86, 116)/Al (100 nm).

To our surprise, even though the thickness of TPA-3FEP varied from 5 to 116 nm, dramatically improved device performances were still obtained in contrast to the control device without a cathode interlayer (Figure 6). Noting that the skeleton of TPA-3FEP is comprised of electron-rich triphenylamine and fluorene units, it is generally known that electrons should not be well transported within it. However, in our current devices, even the thickness of TPA-3FEP reached or surpassed the thickness of the P-PPV layer, electrons still could drift over the thick TPA-3FEP layer and then combine with the holes within the P-PPV emissive layer, and gave green light emission. This could be verified by the EL spectra of these devices. As is shown in Figure S3, Supporting Information, no obvious emission from TPA-3FEP was observed even for the device containing a 116 nm thick TPA-3FEP layer under different current densities before burnout. The original mechanism of how the electrons transport within the thick TPA-3FEP layer is still unclear. We deduce that two

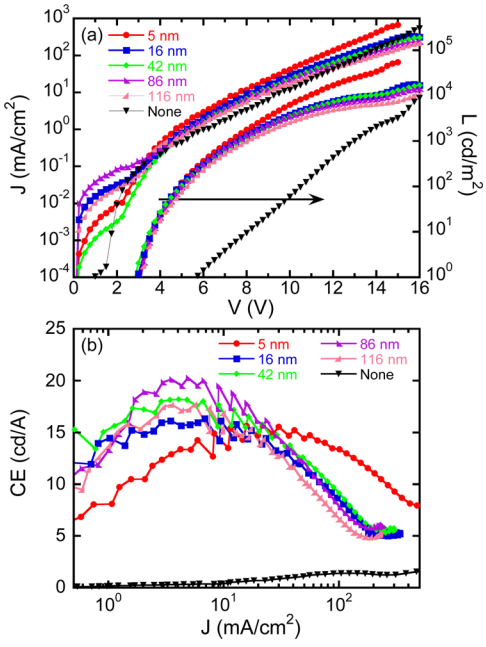

Figure 6. Current density−voltage (J−V) (a) and current efficiency−current density (CE−J) (b) characteristics of the P-PPV-based PLEDs devices with different thicknesses of TPA-3FEP as the cathode buffer layer.

DOI: 10.1021/am507429j
ACS Appl. Mater. Interfaces 2015, 7, 3133−3141

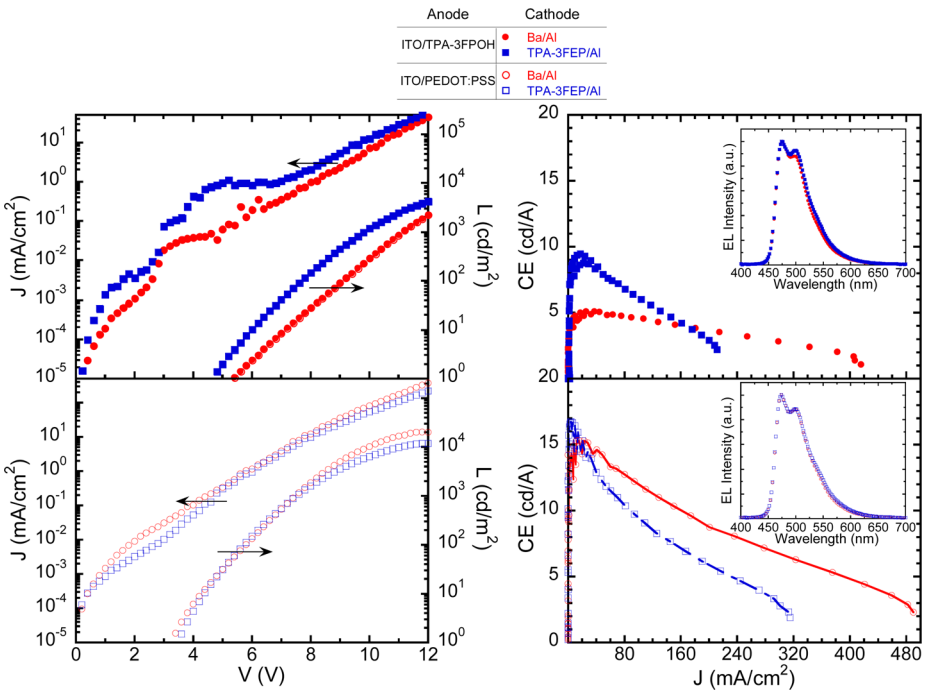

Figure 7. Current density–voltage (J–V) (left) and current efficiency–current density (CE–J) (right) characteristics of the FIrpic-based phosphorescent PLEDs. (Inset) Electroluminescent spectra of the devices.

possibilities should be considered: first, the carrier transport behaviors within some arylamine-containing materials may not be unipolar, electrons may also transport well in these materials comprised of electron-rich arylamine moieties, e.g., Klenkler et al. demonstrated the bipolar transport property of *N*,*N*′-diphenyl-*N*,*N*′-bis(3-methlyphenyl)-[1,1′-biphenyl]-4,4′-diamine (TPD) with similar mobilities for holes and electrons by the time-of-flight (TOF) method.[28] It still could not be confirmed whether TPA-3FEP has bipolar transport behavior, since we failed in obtaining its hole and electron mobilities using general methods like TOF, organic field-effect transistor (OFET), and space-charge-limited current (SCLC). Second, it is also possible that the combination of phosphonate pendants changes the charge transport property of the electron-rich core units and makes the electron transport well within the whole material. In addition, it is still calling for further work to clarify this issue.

Electrode Interlayers for Phosphorescent Light-Emitting Devices. TPA-3FPOH and TPA-3FEP are further applicable as electrode interlayers in phosphorescent PLEDs. Two series of devices were fabricated on the ITO substrates modified by a 5 nm thin TPA-3FPOH layer and a 40 nm thin PEDOT:PSS layer, respectively. A well-established blue phosphorescent light-emitting layer (PVK:OXD-7:FIrpic=70:30:10 in weight, 80 nm) was used to fabricate the devices. Ba (4 nm)/Al (100 nm) and TPA-3FEP (16 nm)/Al (100 nm) were used as the cathode. It is observed that all TPA-3FEP containing devices exhibited higher maximal CE values compared to the corresponding Ba/Al devices based on both the ITO/TPA-3FPOH and the ITO/PEDOT:PSS substrates, though the efficiency roll offs of the former are more obvious (Figure 7). It is worth noting that the maximal CE value of the TPA-3FEP-containing device is about 2 times larger than the Ba-containing device on the ITO/TPA-3FPOH substrates, and the operating voltages of the former are also much lower. The driving voltages of these devices on the ITO/PEDOT:PSS substrates are similar at a luminance below 2000 cd m^{-2}, and the TPA-3FEP containing one showed slightly higher driving voltage at higher luminance. The performances of the devices on the ITO/TPA-3FPOH substrates are inferior in contrast to their counterparts on the ITO/PEDOT:PSS substrates, which is not consistent with the tendency for the P-PPV-based fluorescent PLEDs. This is probably due to the fact that the thin TPA-3FPOH layer may lead to much large leakage current for the FIrpic-based active layer, and the quenching of the triplet excitons may also be more severe compared to the 40 nm thick PEDOT:PSS layer. The EL spectra of these devices are all identical with the emission from FIrpic. These results indicate that these polar solvent-processable trifluorene-substituted triphenylamine derivatives can also be used as electrode interlayers for phosphorescent PLEDs.

CONCLUSIONS

In summary, an effective strategy toward developing efficient electrode interlayer materials was demonstrated based on the peripheral modification of the trifluorene-substituted triphenylamine core. Through rational change of the peripheral pendants, the electron-rich triphenylamine skeleton could be tuned with alternative electron or hole-selective injection or extraction abilities. Their work function tuning abilities on common anode and cathode materials were studied by SKP measurement. Selective carrier injection or extraction abilities of these materials have been explored by the single-carrier devices. Various applications in vacuum- and solution-processed organic light-emitting and photovoltaic devices were thoroughly studied. It was demonstrated that TPA-3FPOH linking the electron-rich trifluorene-substituted triphenylamine core and the peripheral phosphoric acid groups via the sp^3 hybrid alkyl chains could be utilized as a hole injection/extraction material for vacuum- and solution-processed organic light-emitting and photovoltaic devices, whereas TPA-3FEP, whose peripheral polar units are changed

DOI: 10.1021/am507429j
ACS Appl. Mater. Interfaces 2015, 7, 3133–3141

with phosphonate units, exhibited excellent electron injection/extraction abilities, which is contrary to the nature of TPA-3FPOH. Their analogue TPA-3F without any polar units on the periphery keeps the pristine electron-rich nature of the core skeleton and has a good hole transport capacity. The current study provides great meaning to develop high-performance environmentally friendly solvent-processable electrode interlayer materials.

■ ASSOCIATED CONTENT

Supporting Information

UV−vis absorption and PL spectra and CV of TPA-3FPOH, EL spectra of PLEDs with TPA-3FEP as the cathode buffer layer in various thicknesses. This material is available free of charge via the Internet at http://pubs.acs.org.

■ AUTHOR INFORMATION

Corresponding Author

*Tel.: +86-20-22237098. E-mail: mssjsu@scut.edu.cn.

Notes

The authors declare no competing financial interest.

■ ACKNOWLEDGMENTS

The authors greatly appreciate the financial support from the National Natural Science Foundation of China (91233116 and 51073057), the Ministry of Science and Technology (2014CB643501 and 2015CB655003), the Ministry of Education (NCET-11-0159), the Guangdong Natural Science Foundation (S2012030006232), the Department of Education of Guangdong Province (2012KJCX0008), and the Fundamental Research Funds for the Central Universities (2013ZG0007).

■ REFERENCES

(1) Kim, J. S.; Granström, M.; Friend, R. H.; Johansson, N.; Salaneck, W. R.; Daik, R.; Feast, W. J.; Cacialli, F. Indium−Tin Oxide Treatments for Single- and Double-Layer Polymeric Light-Emitting Diodes: The Relation between the Anode Physical, Chemical, and Morphological Properties and the Device Performance. *J. Appl. Phys.* **1998**, *84*, 6859−6870.

(2) Chen, D. C.; Zhou, H.; Cai, P.; Sun, S.; Ye, H.; Su, S. J.; Cao, Y. A Water-Processable Organic Electron-Selective Layer for Solution-Processed Inverted Organic Solar Cells. *Appl. Phys. Lett.* **2014**, *104*, 053304.

(3) Kim, J. S.; Friend, R. H.; Cacialli, F. Improved Operational Stability of Polyfluorene-Based Organic Light-Emitting Diodes with Plasma-Treated Indium-Tin-Oxide Anodes. *Appl. Phys. Lett.* **1999**, *74*, 3084−3086.

(4) Kawano, K.; Pacios, R.; Poplavskyy, D.; Nelson, J.; Bradley, D. D. C.; Durrant, J. R. Degradation of Organic Solar Cells due to Air Exposure. *Sol. Energy Mater. Sol. Cells* **2006**, *90*, 3520−3530.

(5) Wu, S.; Han, S. H.; Zheng, Y. N.; Zheng, H.; Liu, N. L.; Wang, L.; Cao, Y.; Wang, J. A. pH-Neutral PEDOT:PSS as Hole Injection Layer in Polymer Light Emitting Diodes. *Org. Electron.* **2011**, *12*, 504−508.

(6) Shao, J.; Tan, W. Y.; Li, Q. D.; Song, X.; Li, Y. H.; Liu, G.; Mo, Y. Q.; Zhu, X. H.; Peng, J. B.; Cao, Y. Multihydroxylated Aryl Amine as a Novel Alcohol-Processable Hole-Transport Molecular Glass Exhibiting Remarkable Resistance to Weakly Polar Solvents. *Org. Electron.* **2013**, *14*, 2051−2057.

(7) Su, S. J.; Gonmori, E.; Sasabe, H.; Kido, J. Highly Efficient Organic Blue-and White-Light-Emitting Devices Having a Carrier- and Exciton-Confining Structure for Reduced Efficiency Roll-Off. *Adv. Mater.* **2008**, *20*, 4189−4194.

(8) Su, S. J.; Sasabe, H.; Pu, Y. J.; Nakayama, K.; Kido, J. Tuning Energy Levels of Electron-Transport Materials by Nitrogen Orientation for Electrophosphorescent Devices with an 'Ideal' Operating Voltage. *Adv. Mater.* **2010**, *22*, 3311−3316.

(9) Yang, T. B.; Wang, M.; Cao, Y.; Huang, F.; Huang, L.; Peng, J. B.; Gong, X.; Cheng, S. Z. D.; Cao, Y. Polymer Solar Cells with a Low-Temperature-Annealed Sol-Gel-Derived MoOx Film as a Hole Extraction Layer. *Adv. Energy Mater.* **2012**, *2*, 523−527.

(10) Xu, Z.; Chen, L. M.; Yang, G. W.; Huang, C. H.; Hou, J. H.; Wu, Y.; Li, G.; Hsu, C. S.; Yang, Y. Vertical Phase Separation in Poly(3-hexylthiophene): Fullerene Derivative Blends and its Advantage for Inverted Structure Solar Cells. *Adv. Funct. Mater.* **2009**, *19*, 1227−1234.

(11) He, Z. C.; Zhong, C. M.; Su, S. J.; Xu, M.; Wu, H. B.; Cao, Y. Enhanced Power-Conversion Efficiency in Polymer Solar Cells Using an Inverted Device Structure. *Nat. Photonics* **2012**, *6*, 591−595.

(12) Wu, H. B.; Huang, F.; Mo, Y. Q.; Yang, W.; Wang, D. L.; Peng, J. B.; Cao, Y. Efficient Electron Injection from a Bilayer Cathode Consisting of Aluminum and Alcohol-/Water-Soluble Conjugated Polymers. *Adv. Mater.* **2004**, *16*, 1826−1830.

(13) Guan, X.; Zhang, K.; Huang, F.; Bazan, G. C.; Cao, Y. Amino N-Oxide Functionalized Conjugated Polymers and their Amino-Functionalized Precursors: New Cathode Interlayers for High-Performance Optoelectronic Devices. *Adv. Funct. Mater.* **2012**, *22*, 2846−2854.

(14) Duan, C. H.; Wang, L.; Zhang, K.; Guan, X.; Huang, F. Conjugated Zwitterionic Polyelectrolytes and Their Neutral Precursor as Electron Injection Layer for High-Performance Polymer Light-Emitting Diodes. *Adv. Mater.* **2011**, *23*, 1665−1669.

(15) Chen, D. C.; Zhou, H.; Liu, M.; Zhao, W. M.; Su, S. J.; Cao, Y. Novel Cathode Interlayers Based on Neutral Alcohol-Soluble Small Molecules with a Triphenylamine Core Featuring Polar Phosphonate Side Chains for High-Performance Polymer Light-Emitting and Photovoltaic Devices. *Macromol. Rapid Commun.* **2013**, *34*, 595−603.

(16) Zhou, G.; Qian, G.; Ma, L.; Cheng, Y. X.; Xie, Z. Y.; Wang, L. X.; Jing, X. B.; Wang, F. S. Polyfluorenes with Phosphonate Groups in the Side Chains as Chemosensors and Electroluminescent Materials. *Macromolecules* **2005**, *38*, 5416−5424.

(17) He, Z. C.; Wu, H. B.; Cao, Y. Recent Advances in Polymer Solar Cells: Realization of High Device Performance by Incorporating Water/AlcoholSoluble Conjugated Polymers as Electrode Buffer Layer. *Adv. Mater.* **2014**, *26*, 1006−1024.

(18) Zhong, S.; Wang, R.; Mao, H. Y.; He, Z. C.; Wu, H. B.; Chen, W.; Cao, Y. Interface Investigation of the Alcohol-/Water-Soluble Conjugated Polymer PFN as Cathode Interfacial Layer in Organic Solar Cells. *J. Appl. Phys.* **2013**, *114*, 113709.

(19) Li, C. Z.; Chueh, C. C.; Ding, F. Z.; Yip, H. L.; Liang, P. W.; Li, X. S.; Jen, A. K. Y. Doping of Fullerenes via Anion-Induced Electron Transfer and Its Implication for Surfactant Facilitated High Performance Polymer Solar Cells. *Adv. Mater.* **2013**, *25*, 4425−4430.

(20) Zhang, B. H.; Qin, C. J.; Niu, X. D.; Xie, Z. Y.; Cheng, Y. X.; Wang, L. X.; Li, X. L. On the Origin of Efficient Electron Injection at Phosphonate-Functionalized Polyfluorene/Aluminum Interface in Efficient Polymer Light-Emitting Diodes. *Appl. Phys. Lett.* **2010**, *97*, 043506.

(21) Bardecker, J. A.; Ma, H.; Kim, T.; Huang, F.; Liu, M. S.; Cheng, Y. J.; Ting, G.; Jen, A. K. Y. Self-ssembled Electroactive Phosphonic Acids on ITO: Maximizing Hole-Injection in Polymer Light-Emitting Diodes. *Adv. Funct. Mater.* **2008**, *18*, 3964−3971.

(22) Ghaedi, M.; Ansari, A.; Habibi, M. H.; Asghari, A. R. Removal of Malachite Green from Aqueous Solution by Zinc Oxide Nanoparticle Loaded on Activated Carbon: Kinetics and Isotherm Study. *J. Ind. Eng. Chem.* **2014**, *20*, 17−28.

(23) Roosta, M.; Ghaedi, M.; Daneshfar, A.; Sahraei, R.; Asghari, A. Optimization of the Ultrasonic Assisted Removal of Methylene Blue by Gold Nanoparticles Loaded on Activated Carbon Using Experimental Design Methodology. *Ultrason. Sonochem.* **2014**, *21*, 242−252.

(24) Ghaedia, M.; Montazerozohoria, M.; Sajedib, M.; Roostaa, M.; Nickoosiar Jahromib, M.; Asgharic, A. Comparison of Novel Sorbents for Preconcentration of Metal Ions Prior to Their Flame Atomic

DOI: 10.1021/am507429j
ACS Appl. Mater. Interfaces 2015, 7, 3133−3141

Absorption Spectrometry Determination. *J. Ind. Eng. Chem.* **2013**, *19*, 1781−1787.
(25) Vaynzof, Y.; Dennes, T. J.; Schwartz, J.; Kahn, A. Enhancement of Electron Injection into a Light-Emitting Polymer from an Aluminum Oxide Cathode Modified by a Self-assembled Monolayer. *Appl. Phys. Lett.* **2008**, *93*, 103305.
(26) Kepler, R. G.; Beeson, P. M.; Jacobs, S. J.; Anderson, R. A.; Sinclair, M. B.; Valencia, V. S.; Cahill, P. A. Electron and Hole Mobility in Tris(8-hydroxyquinolinolato-N1,O8) Aluminum. *Appl. Phys. Lett.* **1995**, *66*, 3618−3620.
(27) Chen, D. C.; Zhou, H.; Li, X. C.; Liu, M.; Ye, H.; Su, S.-J.; Cao, Y. Solution-Processed Cathode-Interlayer-Free Deep Blue Organic Light-Emitting Diodes. *Org. Electron.* **2014**, *15*, 1197−1204.
(28) Klenkler, A. R.; Voloshin, G. Hole and Electron Transport in Triarylamine-Based Charge-Transport Materials Investigated by the Time-of-Flight Method. *J. Phys. Chem. C* **2011**, *115*, 16777−16781.

DOI: 10.1021/am507429j
ACS Appl. Mater. Interfaces 2015, 7, 3133−3141